Determination of the s-Wave Scattering Length and the C_6 van der Waals Coefficient of ^{174}Yb via Photoassociation Spectroscopy

K. Enomoto,[1] M. Kitagawa,[1] K. Kasa,[1] S. Tojo,[2] and Y. Takahashi[1,3]

[1]*Department of Physics, Graduate School of Science, Kyoto University, Kyoto 606-8502, Japan*
[2]*Department of Physics, Faculty of Science, Gakushuin University, Tokyo 171-8588, Japan*
[3]*CREST, Japan Science and Technology Agency, Kawaguchi, Saitama 332-0012, Japan*
(Received 27 October 2006; published 16 May 2007)

We report photoassociation spectroscopy of ^{174}Yb for the $^1S_0$-$^1P_1$ transition at 1 μK, where only the s-wave scattering state contributes to the spectra. The wave function of the s-wave scattering state is obtained from the photoassociation efficiency, and we determine that the C_6 potential coefficient is 2300 ± 250 a.u. and the s-wave scattering length is 5.53 ± 0.11 nm. Based on these parameters, we discuss the scattering properties of s- and d-wave states.

Photoassociation (PA) of ultracold atoms is a powerful tool for probing vibrational levels of their dimers near the dissociation limit. At a large internuclear distance, typically more than several nanometers, the pair potential of the dimer is excellently expressed by the asymptotic behavior. This simple asymptotic potential is easy to handle and closely related with atomic properties, so that some atomic physical parameters, such as lifetimes of excited states and s-wave scattering lengths, can be deduced very precisely via the PA spectroscopy [1]. The scattering length is of crucial importance for quantitative understanding of properties of quantum degenerate gases and cold collisions.

The scattering length of ytterbium (Yb) atoms is especially important for the following reasons. A Bose-Einstein condensate (BEC) has been successfully achieved for ^{174}Yb, and the Yb BEC attracts a lot of attention because of the unique possibilities offered by its lack of electron spin in the $^1S_0$ ground state and the existence of ultranarrow intercombination transitions [2]. Yb atoms are also intriguing samples for the study of cold collisions, since the interatomic interaction is very simple with no hyperfine structure in the ground state and has many stable isotopes. Analytical theories about rovibrational levels and scattering properties are directly applicable to this system possessing a pure $1/R^6$ asymptotic potential with R the internuclear distance [3,4], and the scattering lengths of all the isotopes are related to one another by a mass scaling law [5]. Yb atoms are also promising candidates for optical frequency standards with the use of the $^1S_0$-$^3P_0$ transition [6–8]. The collisional shift causes one of the major systematic errors with several hertz uncertainty in recent experiments of one-dimensional optical lattice clocks [9,10].

The scattering length of ^{174}Yb is still not accurately known. From the expansion behavior of the BEC, we only inferred that the scattering length of ^{174}Yb should be 6^{+10}_{-5} nm [2]. To accurately determine the scattering

length, PA spectroscopy of ^{174}Yb has previously been carried out for the dipole-allowed $^1S_0$-$^1P_1$ transition at about 100 μK [11]. A node of the scattering wave function of the electronic ground state has intimate relation with the scattering length, and it was only found at about 3 nm. It was expected at that time that the s-wave scattering state mainly contributes to the PA spectra, since this temperature (100 μK) is lower than the height of the centrifugal barrier of the d-wave scattering state. However, a later experiment of PA spectroscopy for the intercombination $^1S_0$-$^3P_1$ transition with rotationally resolved spectra has revealed that the node of the s-wave wave function locates at about 6 nm and the PA signals from the d-wave state are strong comparably to those from the s-wave state even at a low temperature of 25 μK [12]. The existence of a shape resonance has been suggested to explain these unexpectedly strong signals from the d-wave state. It has been pointed out that the existence of the d-wave shape resonance limits the range of the s-wave scattering length [13]. This rough determination of the node position and the existence of the d-wave shape resonance can only provide rough information on the scattering length. The precise node position and the C_6 potential coefficient are needed to accurately determine the scattering length. Note that the potential relevant to the intercombination PA is not represented by an almost pure $1/R^3$ potential and supports only a small number of vibrational states near the dissociation limit, so that the intercombination PA is not suitable for the accurate determination of the scattering length.

In this Letter, we report PA spectroscopy of ^{174}Yb near the $^1S_0$-$^1P_1$ transition at a low temperature of 1 μK where only the s-wave state contributes to the spectra [12]. This experiment not only solves the problem of the seeming discrepancy about the node position described above but also reconstructs the wave function of the s-wave state from the PA rates of different vibrational states [14,15]. By reconstructing the wave function in a wide range of the internuclear distance, we estimate the C_6 potential coeffi-

cient and thus determine the scattering length precisely. The newly determined value of the van der Waals coefficient of Yb atoms must trigger theoretical studies of quantum chemical calculation of lanthanide atoms whose core excitation may contribute strongly. These accurately determined parameters enable us to calculate the scattering properties of some partial waves at nonzero energies. We also quantitatively examine the existence of the d-wave shape resonance, which has been conjectured in the previous work [12].

The experimental procedure to obtain ultracold ^{174}Yb atoms is almost the same as Ref. [2]. Atoms coming from an oven are decelerated by a Zeeman slower with a 399 nm laser for the $^1S_0$-$^1P_1$ transition and are collected by a magneto-optical trap with a 556 nm laser for the $^1S_0$-$^3P_1$ transition. Then the atoms are loaded into a crossed optical trap of a 532 nm laser and are evaporatively cooled down to 1 μK. The number of atoms after evaporative cooling is about 1×10^5, and the peak density is about 3×10^{13} cm^{-3}. A 399 nm laser for PA irradiates the atom cloud and causes loss of atoms. The laser peak intensity I and the irradiation time t are typically 0.1–10 W/cm^2 and 100 ms, respectively. The beam cross section is much larger than the size of the atom cloud. The number of remaining atoms is determined with an absorption imaging method after some time of flight.

The PA spectrum of ^{174}Yb is quite simple. Among four molecular electronic states correlating with the $^1S_0$-$^1P_1$ atomic state, only the $^1\Sigma_u^+$ state is attractive at large R and is accessible from the electronic ground $^1\Sigma_g^+$ state. In addition, ^{174}Yb does not have hyperfine structures. Therefore, all resonances observed correspond to vibrational states supported by a single potential curve. The total angular momentum J_e of these excited states is 1, since only the s-wave scattering is allowed at 1 μK. An example of observed spectra is shown in Fig. 1. In this Letter we count the vibrational quantum number ν' from the dissociation limit. The PA laser power is adjusted so that the atom loss ratio at resonance is roughly the same (about

40%) for each transition to reduce the model dependence of the analysis. We assume that the atom loss is described by an equation $\dot{n} = -K_{\nu'}(I, \nu)n^2 - \Gamma(I, \nu)n$, where n is the density of atoms, $K_{\nu'}(I, \nu)$ is a PA rate coefficient with ν the frequency of the PA laser, and $\Gamma(I, \nu)$ represents one-body loss due to the photon scattering associated with the atomic resonance. The coefficient $\Gamma(I, \nu)$ is measured by comparing atom losses between the cases with and without nonresonant PA light. The solution of this equation is

$$n(t) = \frac{n_0 e^{-\Gamma t}}{1 + \frac{n_0 K_{\nu'}}{\Gamma}(1 - e^{-\Gamma t})}. \quad (1)$$

Since the irradiation time t is long enough compared with the inverses of the trap frequency and the atomic collision rate, we assume that the atom cloud keeps the same density distribution and thus the number of atoms follows the same rate equation. The increase of the temperature due to the PA laser irradiation is at most 0.5 μK, and we ignore its effect on the density distribution. We also assume the coefficient $K_{\nu'}(I, \nu)$ to have a Lorentzian form

$$K_{\nu'}(I, \nu) \propto If_{FC}(\nu')\frac{\gamma(\nu')}{\gamma(\nu')^2 + (\nu - \nu_{\nu'})^2}, \quad (2)$$

where $f_{FC}(\nu')$ is the free-bound Franck-Condon factor, $\gamma(\nu')$ is the linewidth, and $\nu_{\nu'}$ is the center frequency of the resonance. The thermal broadening of the spectra is negligible at this temperature.

The linewidth $\gamma(\nu')$ is found to be a roughly constant value of 0.11 GHz in the range of $\nu' \lesssim 165$. This experimentally obtained width is roughly equal to the sum of the laser frequency jitter and the natural linewidth. However, it abruptly increases with increasing ν' in the range of $\nu' \gtrsim 165$, and it becomes about 0.7 GHz at $\nu' = 175$. The similar behavior was observed in the previous experiment and was considered to be due to predissociation [11]. The quest of this broadening mechanism is beyond the scope of this work. In the following analysis we adopt the data for $\nu' < 165$ with fixing $\gamma(\nu')$ to 0.11 GHz and exclude the data for $\nu' > 165$ because of the large uncertainty of the linewidths.

The Franck-Condon factor $f_{FC}(\nu')$ is obtained through the fitting of the spectra. For a dipole-allowed PA transition, the reflection approximation is excellently good and it claims that [16,17]

$$f_{FC}(\nu') \propto \frac{d\nu'_\nu}{d\nu'}\frac{|\psi_s[R_t(\nu')]|^2}{|\frac{d}{dR}[V_e(R) - V_g(R)]|_{R=R_t(\nu')}}, \quad (3)$$

where $d\nu'_\nu/d\nu'$ indicates the vibrational spacing, $R_t(\nu')$ is the internuclear distance at the classical turning point of the ν'th vibrational state, $V_e(R)$ and $V_g(R)$ are potentials for the electronic excited and ground states, respectively, and $\psi_s(R)$ is the zero-energy wave function of the s-wave scattering state. The classical turning point is determined
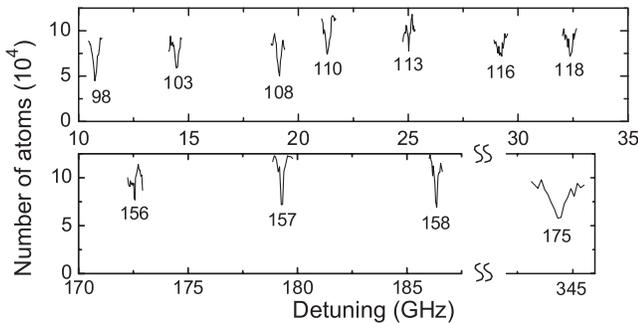

FIG. 1. Example of the observed spectra. The number of atoms after the PA laser irradiation is plotted as a function of the laser frequency detuning from the $^1S_0$-$^1P_1$ atomic resonance. The labels indicate the vibrational quantum numbers ν'.

by assuming a potential form of $V_e(R) = -C_{3e}/R^3 - C_{6e}/R^6$ with the rotational term of $\hbar^2[J_e(J_e + 1) + 2]/2\mu R^2$ with μ the reduced mass, and by using an extended LeRoy-Bernstein formula of Ref. [18]. This potential expression enables us to take advantage of this semiclassical analytical formula about the vibrational level progression. The vibrational number v' assigned in this Letter is obtained with this formula. All the measured resonance frequencies are reproduced within 0.12 GHz accuracy by this formula with three fitting parameters of C_{3e}, C_{6e}, and the noninteger vibrational quantum number at the dissociation limit. We adopt the best-fit parameters of $C_{3e} = 11.535$ a.u. and $C_{6e} = 1.2 \times 10^3$ a.u. This good agreement ensures the validity to use this model potential in the relevant range of 3 nm $\lesssim R \lesssim$ 10 nm, although this potential form does not include the retardation effect. The unknown ground-state potential $V_g(R)$ in Eq. (3) is negligible in the present case. Figure 2 shows the square of the wave function reconstructed from the PA rate coefficient. The error for the ordinate is estimated from the standard deviation of data for a vibrational state with $R_t = 4.2$ nm. Just for a reference, the data for $v' > 165$ are also plotted.

To determine the scattering length a and the C_6 potential coefficient C_{6g} of the ground state, theoretical wave functions are fitted to the experimental data. The wave functions are numerically calculated with the Numerov algorithm for a potential curve $V_g(R) = -C_{6g}/R^6$ and are fitted with fitting parameters of C_{6g}, a, and the amplitude. The best-fit function is achieved with $C_{6g} = 2340$ a.u. and $a = 5.53$ nm, and is shown in Fig. 2 as a solid line. Solid lines in Fig. 3 show contour lines of the chi square χ^2 of the fitting as a function of the parameters C_{6g} and a. The values of χ^2 are relative ones measured from the minimal point. This result is slightly modified by including higher-order potential terms such as C_{8g}/R^8. The C_8 coefficient has been calculated for alkaline earth atoms, and it is on the order of 10^5 a.u. [19]. Although no data of the C_8 coefficient for Yb is available, we assume a conservatively
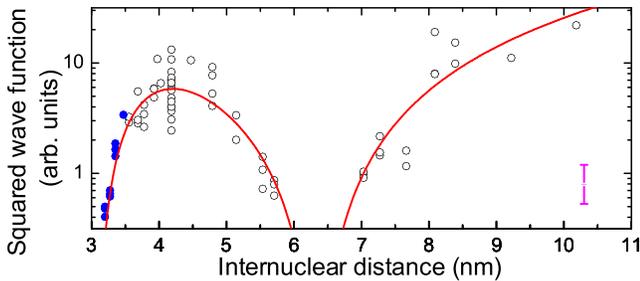
large value of $C_{8g} = 5 \times 10^5$ a.u., and calculate the wave function for a potential $V_g(R) = -C_{6g}/R^6 - C_{8g}/R^8$. This value of C_{8g} corresponds to about 4% of the potential energy at $R = 4$ nm. The result of the fitting with this wave function is also shown in Fig. 3 as dashed lines. We adopt the sum of the areas of $\chi^2 < 1$ for both cases with and without the C_{8g}/R^8 term, and thus conclude that $a = 5.53 \pm 0.11$ nm and $C_{6g} = 2300 \pm 250$ a.u. The last node position is correspondingly 6.34 ± 0.05 nm. The scattering length obtained is 2 orders of magnitude more precise than the value evaluated from the expansion of the BEC [2]. The C_6 coefficient is expressed as a function of oscillator strengths and transition energies of the atom (see, e.g., Refs. [19,20]) and is often estimated approximately from only the contribution of the principal transition. The estimated value from the parameters of the $^1S_0$-$^1P_1$ transition is, however, about 1000 a.u., which is less than half of the experimentally obtained one. It should be noted that the contribution of the principal transition is dominant for alkaline earth atoms [19,20]. Our present study shows that other transitions such as the strong $4f$-$5d$ core excitation must also be considered for the Yb case [21].

Since the potential coefficient and the s-wave scattering length are now determined, the property of other partial wave states can also be discussed. Especially, the d-wave scattering state is important for understanding the results of the previous PA experiments at high temperatures [11,12]. The wave functions and the potential curves for the s- and d-wave states are calculated with the best-fitted parameters of C_{6g} and a and are shown in Fig. 4(a). The energy for both the s- and d-wave wave functions is assumed to be 50 μK, which is rather smaller than the height of the centrifugal barrier (207 μK) for the d-wave state. These non-zero-energy wave functions of the s- and d-wave states are calculated based on the property that the phases of the wave functions are insensitive to the energy and the
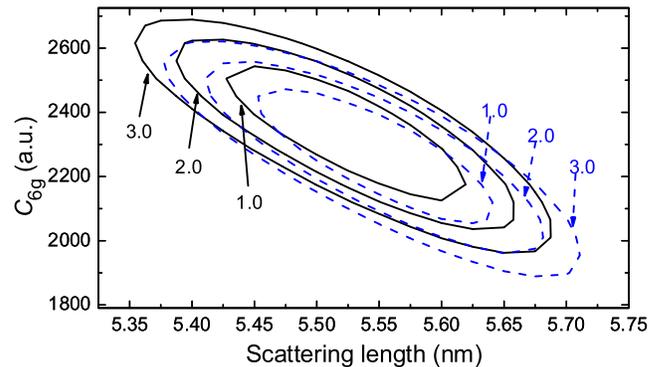

FIG. 2 (color online).   Reconstructed squared wave function of the zero-energy s-wave scattering state. $\bigcirc$ indicate experimental results derived from Eq. (3). The uncertainty of the data is shown at the lower right corner. $\bullet$ representing data for $v' > 165$ are not taken into account for the fitting. The solid line is the best-fitted theoretical wave function with $C_{6g} = 2340$ a.u. and $a = 5.53$ nm.

FIG. 3 (color online).   Contour lines of χ^2 for the fitting of the wave function to the experimental data shown in Fig. 2. This value of χ^2 is measured from the minimal point. The solid lines are the results for the ground-state potential of $V_g(R) = -C_{6g}/R^6$, and the dashed lines are for $V_g(R) = -C_{6g}/R^6 - C_{8g}/R^8$ with $C_{8g} = 5 \times 10^5$ a.u.
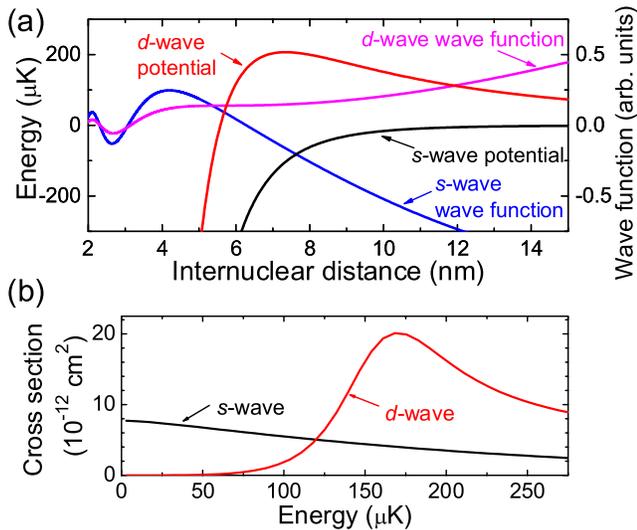
FIG. 4 (color online). (a) Wave functions and potentials of the s- and d-wave scattering states calculated from the best-fitted parameters C_{6g} and a without the C_{8g}/R^8 term. Both the wave functions are calculated for the energy of 50 μK and are normalized to have the same amplitude at $R \rightarrow \infty$. (b) Elastic-collision cross sections of the s- and d-wave scatterings as functions of the collision energy.

angular momentum at $R \ll (2\mu C_{6g}/\hbar^2)^{1/4} \simeq 8$ nm [4]. In the experiment at about 100 μK the PA transition efficiency diminished not at 6.3 nm but at about 3 nm [11]. This fact is explained from the possibility that the PA spectra at that temperature include the contribution from the d-wave scattering state whose wave function does not have a node at 6.3 nm. Note that both the s- and d-wave wave functions have a node at almost the same position of 3 nm, where the rotational term is negligibly smaller than the potential energy $V_g(R)$.

The PA spectroscopy of the intercombination line has shown that the PA signals from the d-wave scattering state of ^{174}Yb are much stronger than those of ^{176}Yb at short internuclear distances and at 25 μK. It was considered that this result implies the existence of a shape resonance for the d-wave scattering state of ^{174}Yb [12]. We calculate the d-wave wave function for various energies and obtain the collisional phase shift. The phase shift changes resonantly at an energy of about 150 μK, and this manifests the existence of a quasibound level there. This shape resonance enhances the amplitude of the d-wave wave function at short internuclear distances. This effect is seen in Fig. 4(a), where both the wave functions have comparable amplitudes at small R even at a low temperature of 50 μK. Figure 4(b) shows elastic-collision cross sections of the s- and d-wave scatterings as functions of the collision energy. The cross section of the d-wave scattering has a peak at about 170 μK due to the shape resonance. The sum of the cross sections is moderately large in a wide range of

the collision energy. This result is consistent with the fast and efficient evaporative cooling, which leads to the achievement of BEC of ^{174}Yb [2]. Note that analytical discussions about general relations among rovibrational levels and scattering properties of partial waves near the threshold have been presented in the framework of the quantum defect theory [4,13,22].

In summary, we have determined the s-wave scattering length of ^{174}Yb precisely as well as the C_6 potential coefficient, based on the PA spectroscopy for the $^1S_0$-$^1P_1$ transition. Collisional properties of the s- and d-wave scatterings at finite temperatures are quantitatively analyzed by using the parameters obtained. As future works, two-color PA spectroscopy will improve the precision of the C_6 coefficient, and similar studies for some other isotopes will reveal the scattering properties of all pair combinations of Yb isotopes.

[1] As reviews, J. Weiner *et al.*, Rev. Mod. Phys. **71**, 1 (1999); K. M. Jones *et al.*, Rev. Mod. Phys. **78**, 483 (2006).
[2] Y. Takasu *et al.*, Phys. Rev. Lett. **91**, 040404 (2003).
[3] B. Gao, Phys. Rev. A **58**, 1728 (1998).
[4] B. Gao, Phys. Rev. A **64**, 010701(R) (2001).
[5] G. F. Gribakin and V. V. Flambaum, Phys. Rev. A **48**, 546 (1993).
[6] H. Katori *et al.*, Phys. Rev. Lett. **91**, 173005 (2003).
[7] C. W. Hoyt *et al.*, Phys. Rev. Lett. **95**, 083003 (2005).
[8] Z. W. Barber *et al.*, Phys. Rev. Lett. **96**, 083002 (2006).
[9] M. Takamoto *et al.*, Nature (London) **435**, 321 (2005).
[10] A. D. Ludlow *et al.*, Phys. Rev. Lett. **96**, 033003 (2006).
[11] Y. Takasu *et al.*, Phys. Rev. Lett. **93**, 123202 (2004).
[12] S. Tojo *et al.*, Phys. Rev. Lett. **96**, 153201 (2006).
[13] P. S. Julienne and B. Gao, arXiv:physics/0609013; P. S. Julienne (private communication).
[14] M. Yasuda *et al.*, Phys. Rev. A **73**, 011403(R) (2006).
[15] P. G. Mickelson *et al.*, Phys. Rev. Lett. **95**, 223002 (2005).
[16] P. S. Julienne, J. Res. Natl. Inst. Stand. Technol. **101**, 487 (1996).
[17] C. Boisseau *et al.*, Phys. Rev. A **62**, 052705 (2000).
[18] D. Comparat, J. Chem. Phys. **120**, 1318 (2004).
[19] J. Mitroy and M. W. J. Bromley, Phys. Rev. A **68**, 052714 (2003).
[20] S. G. Porsev and A. Derevianko, Phys. Rev. A **65**, 020701(R) (2002).
[21] A. Derevianko (private communication).
[22] B. Gao, Phys. Rev. A **62**, 050702(R) (2000).